

# Avalanche dynamics of idealized neuron function in the brain on an uncorrelated random scale-free network

K.E. Lee and J.W. Lee<sup>a</sup>

Department of Physics, Inha University, Incheon 402-751, Korea

Received 1st October 2005 / Received in final form 15 December 2005

Published online 12 April 2006 – © EDP Sciences, Società Italiana di Fisica, Springer-Verlag 2006

**Abstract.** We study a simple model for a neuron function in a collective brain system. The neural network is composed of an uncorrelated configuration model (UCM) for eliminating the degree correlation of dynamical processes. The interaction of neurons is assumed to be isotropic and idealized. These neuron dynamics are similar to biological evolution in extremal dynamics with locally isotropic interaction but has a different time scale. The functioning of neurons takes place as punctuated patterns based on avalanche dynamics. In our model, the avalanche dynamics of neurons exhibit self-organized criticality which shows power-law behavior of the avalanche sizes. For a given network, the avalanche dynamic behavior is not changed with different degree exponents of networks,  $\gamma \geq 2.4$  and various refractory periods referred to the memory effect,  $T_r$ . Furthermore, the avalanche size distributions exhibit power-law behavior in a single scaling region in contrast to other networks. However, return time distributions displaying spatiotemporal complexity have three characteristic time scaling regimes. Thus, we find that UCM may be inefficient for holding a memory.

**PACS.** 05.40.Fb Random walks and Levy flights – 05.45.Tp Time series analysis

## 1 Introduction

The human brain is one of the most complex systems that operate far from equilibrium, which contains trillions of neurons. Typical neurons are made up of dendrites, a cell body, and an axon. Each of these is connected to thousands of other neurons via synapses. Recently, it has been reported experimentally [1] and theoretically [2,3] that the functional structure of the neural network are the “scale-free network” with small-world properties. These show a greater degree of clustering than random networks with no correlations, and have positive degree-degree correlation with assortative mixing. Scale-free networks show a power-law distribution whose degree is defined by the number of links per node. Neuronal activities are also found to exhibit a “self-organized criticality (SOC)”, owing to the fact that the neuronal system is spatially extended with locally interacting units [4–7]. The concept of SOC was originally introduced by Bak, Tang, and Wiesenfeld (who made the BTW model) in 1987 [4]. Nonequilibrium systems are self-organized in the sense that they reach a critical state on their own. The critical state was characterized by a branching process. If the functional network of neurons is in a critical state, it can spontaneously produce neuronal avalanches the same as those of the sandpile in the BTW model and generate spatiotemporal patterns of

activity that can hold a memory of past activity. Lately, Stauffer et al. [2] studied the “Hopfield model” [8] with Hebb coupling between neighbours in a Barabási-Albert (BA) scale-free network [9]. da Silva et al. [10] offered a simple lattice model for ideal brain functioning similar to the Bak-Sneppen (BS) model [5] with the memory effect given by a refractory period,  $T_r$ . The refractory period is the time it takes for an excitable neuron to be stimulated and then be ready for stimulus again. Most recently, the same model was investigated on a small-world network by Lin and Chen [11], where they used networks with rewiring probability generated by Watts-Strogatz [12]. In this paper, according to the scale-free nature of a functional network, we look at neural networks in the human brain as uncorrelated scale-free networks named “uncorrelated configuration model (UCM)” [13] and discuss the simple model for brain functioning the same as introduced in reference [10]. UCM is a scale-free network without degree-degree correlations and clustering correlations. Even though real networks show indeed the presence of correlations, the reason that the uncorrelated networks are valuable is that a test dynamical behavior of the systems with analytic solution is only valid in the absence of correlations. The purpose of our study is to investigate the influences of scale-free network topology on avalanche dynamics and memory effect. We examine the avalanche size distribution with different degree exponents of networks,  $\gamma$  and refractory periods,  $T_r$ . We illustrate

---

<sup>a</sup> e-mail: jaewlee@inha.ac.kr

first and all return time distribution (RTDs) to investigate spatiotemporal correlation of avalanche dynamics at any given values,  $\gamma$  and  $T_r$ . We find our model displays power-law behavior of avalanche size. We notice that the memory effect endowed with refractory time disappears in all scale-free networks. In addition, all critical basic exponents have the same value as the mean field result. RTDs show three characteristic scaling regimes instead of single power-law behaviour, compared with on lattice and small-world networks. The avalanche dynamics on scale-free networks happen frequently at the hub. The hub can easily receive excitatory input signals leading to its firing because of having a greater number of neighbors than a regular lattice case. Thus, the scale-free network may be inefficient for holding a memory.

## 2 Model and simulation method

The modeling of this neuron dynamics is based on networks. The networks are composed of an uncorrelated random scale-free networks. Here, the uncorrelated random scale-free network is known as the uncorrelated configuration model (UCM) [13]. The algorithm of the previous mentioned UCM can be elucidated as follows:

1)  $N$ -nodes are generated by the static method. 2) Each node has  $N_k$  cells with the degree  $k$  satisfying the degree distribution  $P(k) \sim k^{-\gamma}$ . 3) Two cells are randomly selected and connected if they are not linked before. We exclude duplicated connections and self-connections. The network generated by the UCM is not only fully connected but also does not have two type correlations, which are correlations of no two- and three-vertex correlations [13]. Two-vertex correlation is defined as the average number of the degree per nearest neighbors (NN) of the nodes with degree,  $k$ , which is also called degree-degree correlations,  $D_{nn}(k)$ . Three-vertex correlations mean the probability that a node of degree  $k$  forms a loop with two NN. Here, we will refer to three-vertex correlations as clustering correlations [13]. For an uncorrelated property, the following constraints must be satisfied. The degree per nodes,  $k_i$  is subject to the constraint  $m \leq k_i \leq N^{1/2}$ . The number of minimal degree is fixed at  $m = 3$  to prevent alteration of dynamics from a dangling node. The other condition is that the total number of cells is even.

Now, we explain the functional dynamics of neurons as follows. A typical neuron collects signals with the form of an action potential from other neurons through dendrites. The neuron sends out spikes of electrical activity through an axon, which splits into thousands of branches. At the end of each branch, a synapse converts the activity from the axon into electrical effects that inhibit or excite activity in the connected neurons. When a neuron receives excitatory input that is sufficiently large compared with its inhibitory input, it sends a spike of electrical activity into the other neurons. As the consequence of a received signal, the stability of related neurons can be changed. After the release of a spike, the neurons require a period of time to recover. No matter how large the excitatory input may be, the neuron is not allowed to emit a second spike

during the period, which is called the absolute refractory period of the neuron. To capture the main features of all that was stated above, we present the evolution rule of neuron dynamics as follows: each node of the UCM represents a neuron and a link between two nodes stands for a synapse. 1)  $N$  neurons with uniform random numbers between 0 and 1 are distributed over each node. A random number is associated with a barrier  $B_i$ . The barriers are the standard of stability against firing. 2) At each time step, the lowest barrier,  $B_{min}$  is chosen and the neuron is fired by assigning a new random value between 0 and 1. At the same time, the barrier of nearest neighbors are allocated new random values between 0 and 1. The modification of a barrier can be thought of as either the result of the release of a spike by its own neuron or as the consequence of a received signal that changes the stability of the neuron. 3) Last, the updated neuron, as a consequence of firing, is prohibited from firing again during the refractory period,  $T_r$ . However its nearest neighbors can fire at any moment if they have the lowest barrier. Furthermore, if a nearest neighbor is fired within a certain time interval  $t < T_r$ , the barrier of the temporarily frozen neuron is also changed. But it continues to be prohibited to emit a spike until a time,  $t > T_r$  has elapsed.

If this process is iterated the system reaches a critical stationary state by itself, where all the barriers are above the  $B_c$  barrier, a so-called critical threshold. That is, a neural system is self organized, without a tuning parameter, into a stationary state. In the critical state, a neuronal avalanche takes place abruptly in terms of punctuation, i.e each barrier suffers bursts of activity alternating with long periods of calm. This model exhibits intermittent dynamics which resemble the measured results of the firing response of a single neuron in a monkey visual cortex [14]. In our model, we do not attempt to give a detailed description of the elements of the brain. Instead, we express each neuron as a barrier of a uniform random number between 0 and 1 that characterizes its instantaneous probability of releasing a spike, which is the measure of the instability of the neuron. The firing occurs only at a neuron with lowest barrier in time  $t < T_r$ . In this paper, we observe that the system exhibits self-organized criticality.

## 3 Results

In a stationary state, we consider the branching process of avalanche dynamics to be unrestricted by network size corrections [15]. The avalanche is always started from the hub neuron characterized by the node with the largest degree. All neurons with  $B_i > B_0$  are treated as inactive neurons, where  $B_0$  is an auxiliary parameter. The avalanche size of  $B_0(s)$  is defined as the number of the firing sequence less than  $B_0$ . As  $B_0 \rightarrow B_c$ , the avalanche size distribution follows a power-law behavior  $P(S) \sim S^{-\tau}$  with an exponential cutoff. Figure 1 shows avalanche size distribution for the  $B_0(\gamma)$  avalanche with the degree exponents of the networks,  $\gamma = 2.1, 2.5, 2.9, 3.0, 4.0, \text{ and } 5.0$ . The avalanche size distribution follows a power-law behavior,  $P(S) \sim S^{-\tau(\gamma)}$

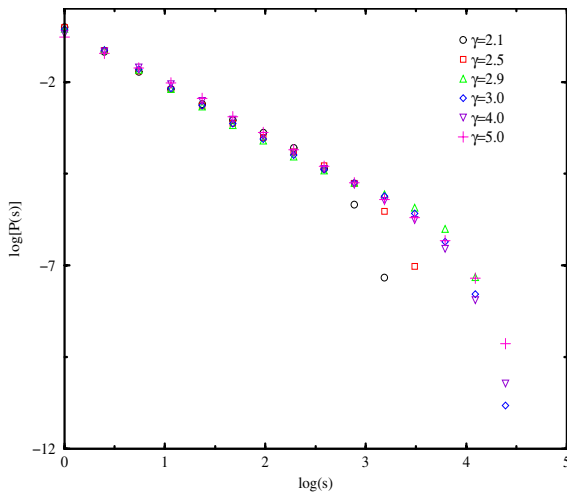


**Fig. 1.** The log-log plot of the probability distribution function  $P(s)$  of the  $B_0(\gamma)$  avalanche size as a function of the avalanche size  $s$  at the critical fitness on UCM for  $\gamma = 2.1, 2.5, 2.9, 3.0, 4.0,$  and  $5.0$  with  $N = 10\,000$ ,  $m = 3$ , and  $T_r = 1$ . The critical threshold barriers are  $B_0 = 0.039, 0.080, 0.121, 0.130, 0.212,$  and  $0.260$  respectively.

extending over a larger regime than other scale-free networks such as the Barabási-Albert (BA) network [9] and the static model introduced by Goh et al. [16]. The more interesting thing is that the power law behaviors of the avalanche size distribution do not exhibit crossover between two different scaling regimes. The avalanche size distribution shows a short intermediate regime and follows an exponential decay at the cut-off regime. The absence of the two regimes in the avalanche size distribution may be explained by the following two reasons. One of the reasons is that an average degree  $\langle k \rangle$  is not fixed with different degree exponent  $\gamma$  as compared with the other static models by Goh's algorithm [16], and in addition is increased as  $\gamma$  gets smaller. The other reason is the absence of the clustering correlations,  $\bar{C}(k)$  as well as degree-degree correlations,  $\bar{D}_{nn}(k)$  [13]. Figure 2 presents the basic critical exponents  $\tau$ , named avalanche size exponent with different  $\gamma$ , where the increment is  $0.1$  in  $2 < \gamma < 3$  and  $0.5$  in  $\gamma > 3$ , at a given  $T_r = 1$ . As we can observe, the critical avalanche size exponent is the same as the mean field result i.e.,  $\tau \simeq 1.5$  for  $\gamma \geq 2.4$ . It is difficult to compare the avalanche size critical exponent  $\tau$  in the UCM with the BA network because the avalanche size distribution of the BA network shows different power-law behavior with two regimes [17,18]. By chance, the critical thresholds are very close to each other,  $f_c = 0.086 \pm 1$  (on UCM) and  $f_c = 0.089 \pm 2$  (on BA) within error bars. Even though it is not a universal value,  $f_c$  seems to be a criterion distinguishing different avalanche dynamics of  $\gamma < 2.4$  from the mean field result of  $\gamma \geq 2.4$ .

In the lattice and small-world network with low rewiring probability  $\phi = 0.01$ , the lévy-flight exponents and the avalanche size exponents increase according to the increment of the refractory period  $T_r$ , respectively. Figure 3 illustrates the probability distribution for the

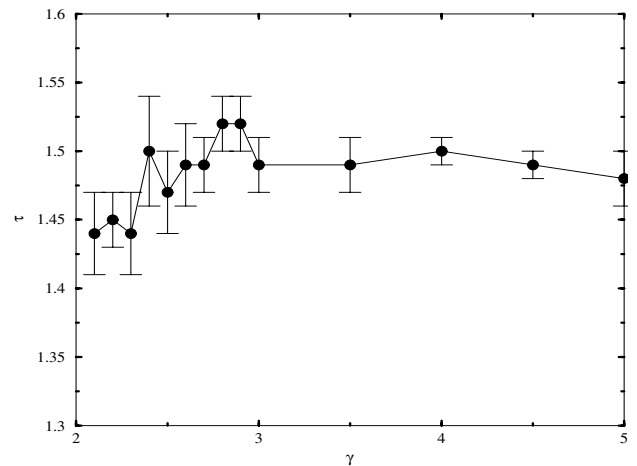


**Fig. 2.** Dependence of the avalanche size exponents as a function of network degree exponents  $\gamma$  with  $N = 10\,000$ ,  $m = 3$ , and  $T_r = 1$ .

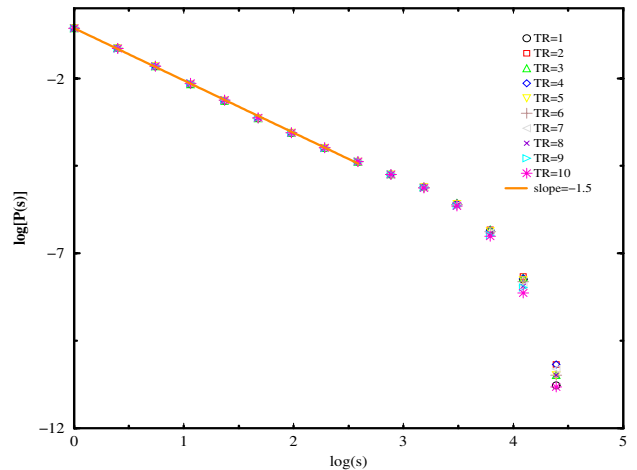


**Fig. 3.** The log-log plot of the probability distribution function  $P(s)$  of the  $B_0(T_r)$  avalanche size as a function of the avalanche size  $s$  at the critical fitness on UCM from  $T_r = 1$  to  $T_r = 10$  with  $N = 10\,000$ ,  $m = 3$ , and  $\gamma = 3$ . The critical threshold barrier is  $B_0 = 0.13$  for all  $T_r$ .

avalanche size on UCM with different  $T_r$  at a given value,  $\gamma = 3$ . At the same time, in Figure 4, we demonstrate the dependency of the exponent  $\tau$  from 1 to 10 with  $B_0 = 0.13$ . All  $\tau$ s are not changed according to varying  $T_r$  unlike the results on lattice or small-world networks [10,11]. In the lattice, the avalanche dynamics of the firing with a larger refractory period are propagated further away from the first firing neuron owing to the fact that the firing is rejected during an elapsed time,  $t < T_r$ . But in the case of the scale-free network, in a stationary state, the activity frequently revisits the hubs with many neighbors and related nodes. Accordingly, the firing neuron is not evolved far from the hub in spite of the large refractory period. For that reason, memory effects in the form of refractory time vanish as the hub is growing larger. Similarly, in the case of small-world networks, if the rewiring probability approaches a threshold eliminating memory

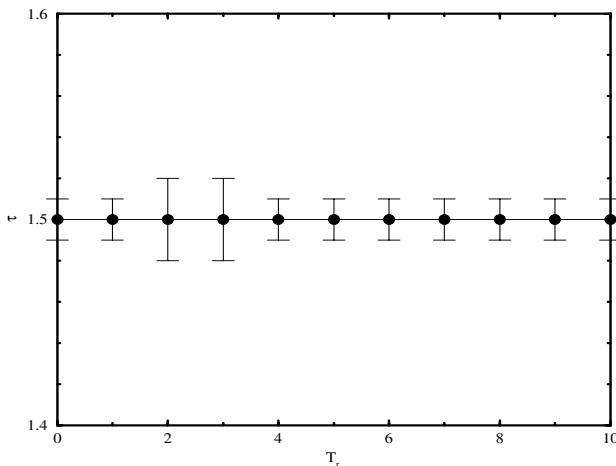


**Fig. 4.** Dependence of the avalanche size exponents as a function of refractory periods  $T_r$  with  $N = 10\,000$ ,  $m = 3$ , and  $\gamma = 3$ .

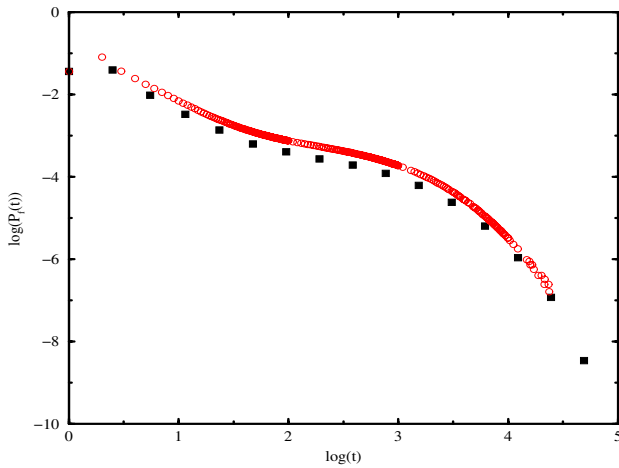


**Fig. 5.** The log-log plot of the probability distribution function  $P(s)$  of the first return time as a function of the time  $t$  at the critical fitness on UCM with  $N = 10\,000$ ,  $m = 3$  at  $T_r = 1$ , and  $\gamma = 3$ . The solid symbols represent the histogram produced, using an exponential bin plot.

effect, the exponent  $\tau$  may also possibly follow the mean-field value with different  $T_r$ .

The probability distribution of first and all return time are valuable quantities for investigating the spatiotemporal correlation and punctuated pattern [4–7, 15]. The first return time with size  $t$  is defined as a separating interval until subsequent activation from a given active neuron. In Figure 5, we present first return time distribution (FRTd) for a fixed values,  $\gamma = 3$  and  $T_r = 1$ . The first return time distribution does not satisfy power-law behavior contrary to the lattice case. The power-law behavior of the early return time region is mostly affected by the dynamics of the hubs. We note that the interval of power-law regime in early return time increases with the degree of the hub. This is because the hubs and nearest neighbors often fire in the ratio of  $k_{hub} + 1$ , where  $k_{hub}$  is the degree of the hub;  $\langle k_{hub} \rangle = 45$  in Figure 5. The intermediate return

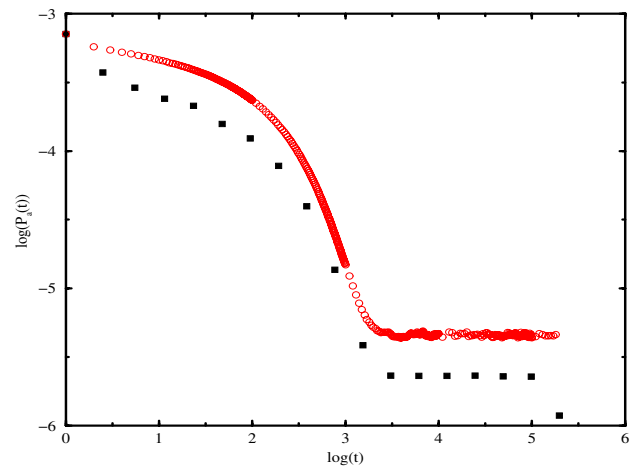


**Fig. 6.** The log-log plot of the probability distribution function  $P(s)$  of the all return time as a function of the time  $t$  at the critical fitness on UCM with  $N = 10\,000$ ,  $m = 3$  at  $T_r = 1$ , and  $\gamma = 3$ . The solid symbols represent the histogram generated, using an exponential bin plot.

time distribution becomes almost constant for all nodes as  $N \rightarrow \infty$ . The reason for this is that each of the nodes has an equal probability of becoming reactive again as there are no correlations for the degrees in UCM. Lastly, in the long return time regime, the slope shows an exponential decay regime with the cut-off for  $t \rightarrow L\xi$  caused by the finite size effect of the dangling node, since the diameter,  $L$  of scale-free network is very small. All return times with size  $t$  are the elapsed time steps regardless of the intermediate firing from firing time  $t_0 = 0$  of a given neuron to time  $t$ . In Figure 6, we plot all return time distributions for fixed values,  $\gamma = 3$ , and  $T_r = 1$ . The all return time distribution (ARTd) is also divided up into three characteristic time scaling regimes. Furthermore, the slope of each regime is small in early return time regimes like the lattice model, but the general scaling relation is not satisfied. The spatio-temporal correlations of all avalanche sizes give rise to the storage of a memory or piece of information [19–22]. A large memory effect may be induced by the scale-invariance. Thus, the absence of scale-invariance of RTDs implies that the memory effect disappears in the scale-free structure of neuronal functioning.

## 4 Conclusion

We have studied a simple model of neuronal functioning in the human brain. With the object of comparing to precedent work, we investigate uncorrelated scale-free networks (UCM) as neural networks instead of more complicated networks with correlations. We find that our model shows a self-organized criticality underlying avalanche dynamics. In the process of simulation, our model displays power-law behaviour of avalanche size without two scaling regimes. At the same time, we find that there are unchangeable avalanche dynamical behaviours for different topologies of the network and various memory effects

with mean field value. We illustrate that RTDs related to spatio-temporal correlations do not show single power-law behaviour. Thus, we can observe that UCM may be inefficient for holding a memory. In future work, complex networks that contain contributions from the memory effect would be required.

The present work has been supported by a research grant of the Asan Foundation.

## References

1. V.M. Eguíluz, D.R. Chialvo, G.A. Cecchi, M. Baliki, A.V. Apkarian, *Phys. Rev. Lett.* **94**, 018102 (2005)
2. D. Stauffer, A. Aharony, L. da F. Costa, J. Adler, *Eur. Phys. J. B* **32**, 395 (2003)
3. C.-W. Shin, S.-H. Kim, e-print [arXiv:cond-mat/0408700](https://arxiv.org/abs/cond-mat/0408700)
4. P. Bak, C. Tang, K. Wiesenfeld, *Phys. Rev. Lett.* **59**, 381 (1987)
5. P. Bak, K. Sneppen, *Phys. Rev. Lett.* **71**, 4083 (1993)
6. H.J. Jensen, *Self-organized criticality: Emergent complex behavior in physical and biological systems* (Cambridge University Press, Cambridge, 1998)
7. P. Bak, *How nature works: the science of self-organized criticality* (Springer-Verlag, New York, 1999)
8. J.J. Hopfield, *Proc. Natl. Acad. Sci. USA* **79**, 2554 (1982)
9. A.-L. Barabási, R. Albert, *Science* **286**, 509 (1999); R. Albert, Barabási, *Rev. Mod. Phys.* **74**, 47 (2002); S.N. Dorogovtsev, J.F.F. Mendes, *Adv. Phys.* **51**, 1079 (2002)
10. L. da Silva, A.R.R. Papa, A.M.C de Souza, *Phys. Lett. A* **242**, 343 (1998)
11. M. Lin, T.-L. Chen, *Phys. Rev. E* **71**, 016133 (2005)
12. D.J. Watts, S.H. Strogatz, *Nature* **393**, 440 (1998)
13. M. Catanzaro, M. Boguñá, R. Pastor-Satorras, *Phys. Rev. E* **71**, 027103 (2005)
14. C. Koch, *Nature (London)* **385**, 207 (1997)
15. M. Paczuski, S. Maslov, P. Bak, *Phys. Rev. E* **53**, 414 (1996)
16. K.-I. Goh, B. Kahng, D. Kim, *Phys. Rev. Lett.* **87**, 278701 (2001); D.-S. Lee, K.-I. Goh, B. Kahng, D. Kim, *Nucl. Phys. B* **696**, 351 (2004)
17. S. Lee, Y. Kim, *Phys. Rev. E* **71**, 057102 (2005)
18. N. Masuda, K.-I. Goh, B. Kahng, e-print [arXiv:cond-mat/0508623](https://arxiv.org/abs/cond-mat/0508623)
19. J.M. Beggs, D. Plenz, *J. Neurosci.* **23**, 11167 (2003)
20. J.M. Beggs, D. Plenz, *J. Neurosci.* **24**, 5216 (2004)
21. L. de Arcangelis, H.H. Herrmann, C.P. Capano, e-print [arXiv:q-bio.NC/0411043](https://arxiv.org/abs/q-bio.NC/0411043)
22. C. Haldeman, J.M. Beggs, *Phys. Rev. Lett.* **94**, 05810 (2005)